American Journal of Water Resources, 2016, Vol. 4, No. 1, 1-15
Available online at http://pubs.sciepub.com/ajwr/4/1/1

DOI:10.12691/ajwr-4-1-1

Hydrologic and Hydraulic Impact of Climate Change on Lake Ontario Tributary

Sadik Ahmed, Ioannis Tsanis*

Department of Civil Engineering, McMaster University, 1280 Main Street West, Hamilton, Ontario L8S 4L7, Canada
*Corresponding author: tsanis@mcmaster.ca

Abstract Climate model projections indicate that the frequency and magnitude of hydrological extremes will increase in a future climate due to increasing concentration of greenhouse gases. Increase in precipitation depth will lead to higher peak flows, and will bring floods with higher inundation depths and larger extends. This study involves the climate change impact analysis of design storms, peak flows and flooding scenario for the Clearview Creek drainage area located in Southern Ontario, Canada. First, the storm depths for different return periods and durations were calculated from the observed rainfall data and the North American Regional Climate Change Assessment Program (NARCCAP) climate simulations. The storm depths were calculated by using the best fitted distribution among twenty seven distributions. The design storm depths calculated from the observed and climate model simulated data are used as input into an existing Visual OTTHYMO model of the study area for flow simulation. The simulated peak flows for 24hr Storm of different return periods are used as input in the HEC-RAS model for hydraulic analyses. Frequency analysis results show that the storm depths are predicted to increase significantly under future climate. Simulated flow results show an increase of peak flows ranging from about 26 % to 64% for 2yr and 100yr return periods at the outlet of the Creek. Finally, the analyses of flooding scenario revealed an average increase of water surface elevation and extents by 30 cm and 37.1 m, respectively, for a 100 year return period flood. It is also revealed that the variability of flow simulated by hydrologic model and flow area simulated by the hydraulic analyses tool are much higher than the variability of the storm depths under future climate condition.

Keywords: *climate change, frequency analysis, design storm, hydrology, flood, Canada*

Cite This Article: Sadik Ahmed, and Ioannis Tsanis, "Hydrologic and Hydraulic Impact of Climate Change on Lake Ontario Tributary." *American Journal of Water Resources*, vol. 4, no. 1 (2016): 1-15. doi: 10.12691/ajwr-4-1-1.

1. Introduction

The anthropogenic gas emissions is now higher than ever, and more than half of the observed increase in global average surface temperature from 1951 to 2010 was caused by the anthropogenic increase in GHG concentration and other anthropogenic forcing together [25]. Climate change studies revealed that warming trends are linked to global hydrological cycle [1], such as increase in extreme precipitation [10,32]. The potential increase of rainfall events can lead to an increase in rain generated flood [1,31,45,50,51]. Flood is one of the greatest natural disasters to human society and it severely affects the social and economic development of a country. Its adverse impact includes loss of life and property, environmental degradation and shortage of food, energy, water and other basic needs. Flood management strategy continuously evolved in many flood prone countries over time. The flood management strategy has gradually shifted from narrow focus on structural flood control measures to a combination of structural and non-structural flood control measures and further to Integrated Flood Management (IFM). Flood risk map is one of the effective non-structural measures widely used by many countries around the world. In Canada, the federal government in conjunction with provinces invested millions of dollars to control flood by building structural measures in 1950s, 1960s and 1970s. But after the extensive flood damage across Canada in the early 1970s, it was realized that prevention of flood and non-structural measures are needed to reduce flood damage. This realization made the federal government to initiate the Flood Damage Reduction Program [16]. The main activities under this program are identifying, mapping and designating flood risk area and then applying policies to discourage development in the flood risk area. After designation of flood risk area, both federal and provincial governments do not build or support any flood vulnerable development in such areas. The flood standards used to define flood limit in Ontario are (i) flood resulted from a rainfall actually experienced during a major storm such as the Hurricane Hazel storm that struck Southern Ontario on October 15, 1954 (ii) 100 year return period flood and (iii) an observed flood event, and 100 year flood is the minimum acceptable regulatory flood standard [46]. The regulatory flood limit for Clearview Creek, the study area for this study, is the water level produced by a 100 year return period flood. In absence of adequate streamflow records, rainfall data is used to simulate stream flows. When flow is simulated from a specific return period

storm, the commonly made assumption is that storm of a specific frequency produces streamflows of the same frequency. Credit Valley Conservation uses a 24 hour 100 year return period storm depth for flood mapping study for this study area. The storm depths are calculated from the historic rainfall time series without consideration of climate change impact. This study aims to investigate the climate change impact on hydrological processes by analyzing storm depths and storm flows, and impact on hydraulics by analyzing water level and flooding scenario addressing the climate change impact.

The design storm depths are calculated employing statistical analyses on observed rainfall time series based on the assumption of a stationary climate, but the Earth is now in a nonstationary climate [3,27,38]. Owing to this nonstationary, sustainability of non-structural flood management measures such as flood mapping would benefit from calculating storm depth addressing the climate change impact. A number of studies have been conducted recently to calculate storm depths of different duration and return period addressing the impact of climate change, but maximum three probability distributions were used to fit the annual maximum precipitation time series for calculating storm depths by employing frequency analysis. As example, [39] used the Log-Pearson Type III, some studies [17,35] used generalized extreme value, [56] used Extreme value type I (EV I), [55] used Gumbel and generalized extreme value for storm depth calculation. Considering the importance of selection of probability distribution, twenty seven distributions were tested using two statistical tests for observed, NARCCAP current and future datasets, and the best fitted distribution was used for frequency analysis to calculate design storm depths.

The North American Regional Climate Change Assessment Program (NARCCAP) provides high resolution climate scenarios created from multiple GCMs and RCMs to facilitate climate change impact assessment. Climate change impact study using climate model simulations should consider multiple projections to address the inherent uncertainty in climate projections [37]. In this study, six RCM+GCM pairs provided by NARCCAP were used for storm depth calculation to address the uncertainty in the climate projections. The precipitation dataset from NARCCAP are available as gridded data, and are areal average not point estimates [4]. Some studies applied delta change factors to precipitation time series [e.g., [2,45,48,49]], and others applied it to design storm depth [17,56]. The delta change method was applied to transpose design storm depth calculated from gridded NARCCAP data to Toronto Pearson Airport meteorological station to remove the systematically difference between climate model simulated and observed precipitation.

Climate change impact on river/stream flow has been investigated by a number of researches using different climate model simulations in the last decades, most of the study focused on continuous simulation of river flow for comparatively big and rural catchments [52,53]. There are very few studies which investigated the impact of climate change on storm flow in urban areas using design storm as input in an event-based hydrologic modeling tools. However, studies investigated the effect of climate change on urban-catchment scale storm water runoff using long-term simulation revealed significant increase of peak flows in different areas. [54], for example, found a significant increase up to 80% for the average peak flows under climate change scenarios of 2030-2059 in the Bronx River watershed in New York City. The increase of peak flow will heighten the flood risk under future climate condition. [14] reported that, under future climate, the extent of flood will be larger and will increase the level of risk to public infrastructure in the Upper Thames River basin in Canada. They also indicated insignificant differences of flood lines between current and future scenario for 100 yr return period flood due to steep slope in some areas, despite the difference in water surface elevation of approximately 40cm. This study used a single event hydrologic model simulation software Visual OTTHYMO for flow simulation and a hydraulic modeling tool - the Hydrologic Engineer Center's River System Analysis System (HEC-RAS) software for flooding scenario analyses. To achieve the objectives, the following main activities were carried out in this research: performing frequency analyses to compute storm depths for observed, NARCCAP current and future datasets; transposing design storm depth calculated from gridded NARCCAP data to Toronto Pearson Airport meteorological station using delta change factor; simulation of peak flows for different return period using the Visual OTTHYMO rainfall runoff model; simulation of hydraulic metrics using HEC-RAS hydraulic model; and analyses of storm depths, flows and flooding scenarios under current and future climate conditions.

2. Study Area and Data

2.1. Study Area

The study area, Clearview Creek drainage area which is under the jurisdiction of Credit Valley conservation, is located mostly in the City of Mississauga and also in the Town of Oakville, Southern Ontario, Canada. The study area has undergone significant urban growth in recent years, and the climate of this area can be characterised by humid-continental. The climate of the study area is represented by the meteorological data of Pearson International Airport station. Based on the meteorological data from 1981 to 2010 observed at Toronto Lester B. Pearson International Airport, the daily average temperature over the year is 8.2°C. The extreme maximum temperature 38.3°C and minimum temperatures - 31.3 °C were observed on 25 August 1948 and 4 January 1981, respectively. The total yearly precipitation, rainfall and snowfall at this area are 785.9 mm, 681.6 mm and 108.5 cm respectively based on the data from 1981-2010 [13]. The total area draining from the Clearview Creek drainage area to the Lake Ontario is about 478.66 ha.

2.2. Observed Meteorological Data

This study used the rainfall time series for 30 years, from 1971 to 2000, observed at Toronto Lester B. Pearson International Airport meteorological station with a latitude and longitude of 43°40'38.000" N and 79°37'50.000" W respectively. The hourly observed rainfall time series were obtained from Ontario Climate Center, Environment Canada. The Intensity-Duration-Frequency curves used by

city of Mississauga and Credit Valley Conservation for development studies for the study area were originally derived from the observed rainfall data taken from the Pearson International Airport. Therefore, the observed rainfall data at this meteorological station were used to calculate the design storm depths for observed/baseline scenario in this study.

2.3. NARCCAP Climate Data

This study used the climate data sets collected from the North American Regional Climate Change Assessment Program [36,37,44]. NARCCAP is a coordinated multi-model numerical experiment [37] that provides climate projections for several RCM+GCM pairs at similar spatial resolutions over identical periods covering the conterminous United States and most of Canada. It provides all the data at a gridded horizontal resolution of 50km and time span 33 years for both current (1968-2000) and future (2038-2070) period. The first three years of data, spin-up periods [34] has been discarded in this study. NARCCAP data permits assessment of climate change impact by comparing the climate of mid twenty-first century with that of twentieth century. Every future simulation in NARCCAP follows greenhouse gas and aerosol concentration based on A2 emission scenario described in the Special Report on Emissions Scenarios (SRES) [43]. The data are stored in the NetCDF files in 2D arrays and array dimensions are named "xc" and "yc" within the file. The array dimensions (yc, xc) of nearest point of Toronto Lester B. Pearson International Airport found from the grid cell maps for CRCM, HRM3 and RCM3 are (52,100), (59, 105) and (45, 94) respectively.

The precipitation time series of temporal resolution 3 hour provided by six different RCM+GCM pairs were used in this study. These six pairs includes three RCMs and four GCMs, the RCMs are Canadian Regional Climate Model (CRCM) [42], Hadley Regional Model 3 (HRM3) [26] and Regional Climate Model version 3 (RCM3) [12,20], and the GCMs are Community Climate System Model (CCSM) [8], Third Generation Coupled Global Climate Model (CGCM3) [15], Geophysical Fluid Dynamics Laboratory GCM (GFDL) [19] and Hadley Centre Coupled Model, version 3 (HADCM3) [21,47]. The six RCM+GCM pairs' data used in this study are CRCM+CCSM, CRCM+CGCM3, HRM3+GFDL, HRM3+HADCM3, RCM3+CGCM3 and RCM3+GFDL.

3. Methodology

The procedure used in this study involves (1) storm depths calculation under current and future climate condition; (2) transforming storm depths into runoff using a hydrological model, and (3) transforming runoff into water surface elevation required to develop flooding scenario under current and future climate condition using a river system analyses tool.

3.1. Design Storm

Table 1. Best fitted distribution for NARCCAP data for different duration [Case 1 (current x, future √), case 2 (current *, future +)]

	CrcmCcsm				CrcmCgcm3				Hrm3Gfdl				Hrm3Hadcm3				Rcm3Cgcm3				Rcm3Gfdl			
Distribution	3	6	12	24	3	6	12	24	3	6	12	24	3	6	12	24	3	6	12	24	3	6	12	24
Normal	x	x											√		√	x						x		
LogNormal						+	√		x			x												
Galton																*								
Exponential				x					√	x														x
Gamma						x	x							√	*				+					
Pearson III													+											
LogPearson III																		+		+		+		
Gumbel EV 1 Max	*√		x√		√	√		√						x					x√				x	
EV2-Max		√+						x									x√	*		x√	√			√
Gumbel EV 1 Min																								
Weibull										√			*											
GEV Max																								
GEV Min		*					+															*		
Pareto			+							*	+					+								
L-Moments Normal											x		x		x				*	*				
L-Moments Exponential				√												√								
L-Moments EV1 Max					x			+						*									*	
L-Moments EV2 Max	+											√					*	√						+
L-Moments EV1 Min																								
L-Moments EV3 Min																								
L-Moments GEV Max												+									+			*
L-Moments GEV Min			*	*+	+	*	*		*+	+	*√	*		+			+				*			
L-Moments Pareto					*										+						x			
GEV-Max (k spec.)								*										x				√	+	
GEV-Min (k spec.)																								
L-Moments GEV-Max (k spec.)																							√	
L-Moments GEV-Min (k spec.)																								

Design storm depths were calculated for different duration (3h, 6h, 12h and 24h) and six different return periods (2yr, 5yr, 10yr, 25yr, 50yr and 100yr) for historic observations and climate model simulations for current

and future period. NARCCAP provided precipitation time series of 3h resolution were aggregated into 3-, 6-, 12- and 24 h duration on an annual basis. Then time series of annual maximum rainfall depth were generated by determining the yearly maximum value for each duration from the aggregated time series. Frequency analysis was performed on these annual maximum time series data of each duration to calculate storm depths. Two tests, Pearson chi-square test and Kolmogorov-Smirnov, were used to test the goodness of fit of each distribution among twenty seven distributions as shown in Table 1. Environment Canada uses Gumbel Extreme Value distribution to fit the annual extremes of rainfall for the study area for developing IDF curves. Therefore, Extreme Value type 1 (EV1) was used for frequency analyses together with the best fitted distribution. Each distribution was tested for its goodness of fit following the attained percentage of the parameter "a", and the distribution that attained the highest percentage of a for a particular time was selected for frequency analyses for that time series.

The percentage value of 'a' for Chi-square test (equation 1) and Kolmogorov-Smirnov (equation 2) are defined by the following two equations:

$$a_{attained} = 1 - x^2(m = k - r - 1, q) \quad (1)$$

$$a_{attained} = 1 - x^2(m, q) \quad (2)$$

where m are the degrees of freedom of chi square test, k is the number of bins used in chi square test, r is numbers of parameters of the distribution and q is the Pearson parameter. The theoretical background of the tested distributions is presented in [30]. A statistical analysis software, Hydrognomon [30], was used to find the best fitted distribution among 27 statistical distributions.

Three sets of storm depth were calculated for historical observation, NARCCAP current and future simulations. The three sets are: (1) Case 1: storm depth with best fitted distribution tested by Chi-square test (2) Case 2: storm depth with best fitted distribution tested by Kolmogorov-Smirnov, and (3) Case 3: storm depth with Extreme Value type 1 (EV1).

All the NARCCAP dataset are provided at grid scale, therefore storm depth values calculated from the NARCCAP datasets are for grid scale. The bridging of the gridded climate change projections with the historic observation at meteorological station is essential for climate change impact study at watershed scale. Delta change factor can be applied to discrete totals i.e. design storm depths [17] to estimate future rainfall intensities at the station scale from the estimated values at the model grid-scale (both current/historic and future) and at the observed station scale (current/historic). The assumption in transposing projected future change in climate onto point observation is that the areal-to-point relationships of precipitation remain constant in future climates [35]. The delta change factor application procedure (presented by equations 3, 4 and 5) described by [56] was used to produce future station-scale intensities/depths:

$$I_F^{(g)} = I_H^{(s)} 1 + \Delta_{F-H}^{(g)}(T, d) \quad (3)$$

$$\Delta_{F-H}^{(g)}(T, d) = \frac{I_F^{(g)}(T, d) - I_H^{(g)}(T, d)}{I_H^{(g)}(T, d)} \quad (4)$$

$$I_F^{(s)}(T, d) = I_H^{(s)}(T, d) \frac{I_F^{(g)}(T, d)}{I_H^{(g)}(T, d)} \quad (5)$$

Where, T and d denote return period and duration respectively, H and F denote historic and future, and s and g denote station and grid respectively.

Delta change factor was applied to all NARCCAP datasets to produce storm depths at station scale under future climate condition, and the results are presented in the Table 2.

Two traditionally derived storms have been traditionally adopted as representative storm, namely the SCS Type II and Chicago distribution [41]. Credit Valley Conservation uses 24hr Chicago storm distribution for hydrologic modeling for flood line delineation in the study area. The Chicago storm was developed by C.J. Keifer and H.H. Chu [28] on 25 years of rainfall record for the city of Chicago. The storm is generally applied to urban basins where peak runoff rates are largely influenced by peak rainfall intensities. Design storm depths to be used in the hydrologic model were discretized using Chicago distribution for a time step of 10 minutes. The peak intensity for the storm is computed using the following equation:

$$I_p = \frac{A}{(\Delta t + B)^C} \quad (6)$$

The 10-minute intensities are then distributed around the peak as rΔt before the peak and (1-r) Δt after the peak. MTO suggested using an r value of 0.38 for all MTO districts to provide a consistent application across the province. The IDF parameter values A, B and C were obtained from the IDF equation used by City of Mississauga [5]. The IDF parameters are presented in the Table 3. The intensities before and after the peak were calculated using the following equations:

Before the peak:

$$\int_{t_{b1}}^{t_{b2}} i_b dt_b = \left[\frac{A t_b}{\left([t_b / r] + B \right)^c} \right]_{t_{b1}}^{t_{b2}}. \quad (7)$$

After the peak:

$$\int_{t_{b1}}^{t_{b2}} i_a dt_a = \left[\frac{A t_a}{\left([t_a / (1-r)] + B \right)^c} \right]_{t_{a1}}^{t_{a2}} \quad (8)$$

Where, i_a and i_b are intensities, t_b is the time after the peak intensity in minute, t_a is the time after the peak intensity in minute, A, B and C are IDF parameters. A sample calculation can be found in MTO Drainage Management Manual [41].

Discretized design storms for 24hr duration and 2, 5, 10, 25, 50 and 100 year return period were developed using Chicago distribution and IDF parameter listed in the Table 3. The temporal distribution of the six return period developed using theses IDF parameters were used for both observed and NARCCAP storm depths for the study area. A sample discretized storm for 24 hour and 100 year return period return period is sown in the following Figure 1.

Table 2. Design storm depths (in mm) calculated from observed data and NARCCAP future datasets

Return Period	Duration (h)	Observed			CrcmCcsm			CrcmCgcm			Hrm3Gfdl		
		Case 1	Case2	Case3	Case 1	Case2	Case3	Case 1	Case2	Case3	Case 1	Case2	Case3
2yr	2	30.4	30.4	29.9	32.8	32.9	33.6	33.1	33.8	32.5	33.3	35.1	34.7
	6	34.2	34.6	35.3	33.4	34.3	36.6	36.5	38.5	38.5	46.4	40.8	43.4
	12	37.9	38.3	40.1	38.4	38.9	40.7	42.2	42.1	44.1	46.2	48.7	53.6
	24	45.3	44.0	46.2	49.7	50.5	51.1	50.3	48.7	50.5	57.8	57.0	63.4
5yr	2	39.8	39.8	39.1	42.1	42.2	42.5	40.1	39.6	39.6	45.0	45.8	45.6
	6	46.9	47.6	49.0	45.6	46.1	50.2	48.7	50.4	51.9	64.8	58.1	63.3
	12	53.5	52.0	55.0	53.5	52.5	55.0	57.1	54.9	58.6	73.2	72.9	78.3
	24	58.7	57.5	61.8	64.8	63.4	67.1	66.2	65.2	67.4	81.6	79.5	92.8
10yr	2	45.4	45.4	45.2	49.2	48.9	49.0	43.9	43.2	44.2	53.2	52.3	52.9
	6	56.5	57.0	58.1	56.5	56.4	59.4	58.9	58.4	60.8	74.8	74.0	76.5
	12	65.0	63.1	64.9	64.5	46.7	64.4	67.5	65.4	67.9	97.1	93.5	94.9
	24	68.9	69.0	72.1	76.5	73.6	77.4	77.0	77.9	78.5	104.6	103.2	113.1
25yr	2	52.0	52.0	52.9	58.3	57.4	56.5	48.4	48.1	50.2	63.2	60.1	62.1
	6	70.4	69.9	69.6	75.3	73.0	70.7	74.5	69.7	72.0	87.0	100.1	93.6
	12	80.1	79.6	77.3	79.0	77.6	76.2	80.8	81.5	79.5	132.7	123.6	116.1
	24	83.7	86.6	85.2	93.0	91.6	87.6	91.1	95.8	92.7	145.2	147.2	138.8
50yr	2	56.5	56.5	58.6	65.6	64.3	62.5	51.2	52.0	54.3	70.0	65.5	68.9
	6	82.0	80.3	78.1	92.3	87.7	79.3	87.7	79.2	79.9	96.1	123.8	106.1
	12	91.4	94.0	86.6	89.8	89.4	85.1	90.4	95.3	88.0	162.1	149.5	132.1
	24	96.0	102.3	94.8	107.1	105.2	96.5	101.4	110.5	103.0	185.9	194.0	157.8
100yr	2	60.7	60.7	64.3	72.5	71.9	68.2	53.9	55.8	58.6	76.2	70.6	75.7
	6	94.8	91.2	86.5	114.8	106.8	88.0	102.9	88.8	87.9	105.6	151.0	118.5
	12	102.7	110.1	95.8	100.4	101.7	93.7	99.9	110.9	96.5	193.6	177.8	148.2
	24	109.6	120.5	104.4	122.4	116.3	109.9	111.9	126.2	113.5	238.7	256.8	176.8
Return Period	Duration (h)	Hrm3Hadcm3			Rcm3Cgcm3			Rcm3Gfdl					
		Case 1	Case2	Case3	Case 1	Case2	Case3	Case 1	Case2	Case3			
2yr	2	26.6	26.4	26.5	42.7	40.8	42.5	36.0	34.9	37.0			
	6	33.4	33.1	33.8	42.3	44.7	46.9	40.3	41.6	44.7			
	12	38.3	38.9	40.8	48.4	47.4	51.2	46.3	47.0	50.0			
	24	41.5	43.6	47.8	56.3	52.0	57.8	57.8	54.0	57.5			
5yr	2	33.4	32.7	32.8	57.8	64.3	59.1	46.8	46.5	52.9			
	6	43.3	44.5	44.3	64.9	71.2	72.5	58.0	58.4	65.0			
	12	52.4	53.2	53.6	73.3	71.1	75.4	61.5	59.3	64.6			
	24	58.4	60.7	64.3	75.1	72.8	80.2	71.6	69.8	76.7			
10yr	2	37.5	37.0	37.0	67.6	77.6	70.0	57.3	57.4	63.8			
	6	50.3	52.1	51.4	85.2	91.3	89.9	74.5	73.8	78.6			
	12	63.1	62.4	62.1	91.9	91.1	91.7	73.6	70.3	73.9			
	24	74.8	74.4	75.2	89.6	92.8	95.2	82.5	84.5	89.3			
25yr	2	42.5	42.6	42.5	79.7	89.0	83.4	76.0	76.4	77.5			
	6	60.0	61.6	60.2	119.6	119.1	111.8	102.5	99.6	96.1			
	12	77.0	73.3	72.7	116.7	121.9	112.6	90.9	88.2	85.6			
	24	101.0	93.5	89.0	111.5	126.2	114.2	100.1	109.0	105.3			
50yr	2	45.9	46.6	46.6	88.6	93.4	93.5	94.1	95.5	87.5			
	6	67.9	69.0	66.8	153.4	141.0	128.1	129.6	124.3	109.0			
	12	87.4	81.7	80.7	135.5	149.6	128.3	105.2	104.9	94.2			
	24	124.5	109.0	99.0	130.1	158.2	128.3	116.3	132.2	117.1			
100yr	2	48.9	50.6	50.6	97.3	94.9	103.4	116.7	120.1	97.4			
	6	76.3	76.1	73.3	195.6	163.6	144.3	163.2	154.1	121.8			
	12	97.8	90.1	88.4	154.2	181.3	143.8	120.9	125.1	102.7			
	24	151.7	125.6	109.1	151.2	197.6	142.3	135.8	160.9	128.9			

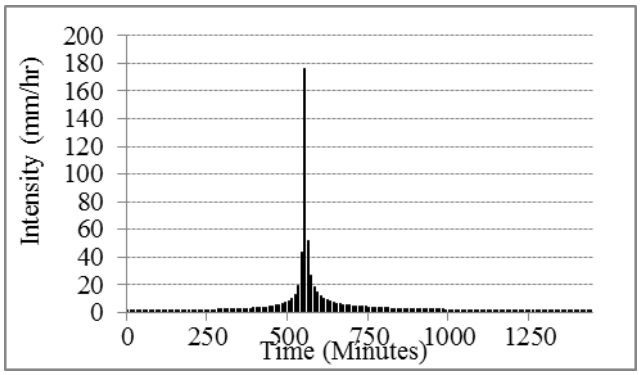

Figure 1. Chicago storm of 24 hr 100 year for city of Mississauga IDF parameters

Table 3. IDF Parameters of City of Mississauga IDF Curves

Parameter	Return Period					
	2	5	10	25	50	100
A	610	820	1010	1160	1300	1450
B	4.6	4.6	4.6	4.6	4.7	4.9
C	0.78	0.78	0.78	0.78	0.78	0.78

3.2. Hydrologic Modeling

The most widely used approach to simulate hydrological impact of climate change is done by inputting climate projections into a deterministic or conceptual hydrological model that contains physically based mathematical descriptions of hydrologic phenomena

[11,18,22,29,33]. Precipitation data can be inputted into the hydrologic model in a form of continuous time series data or event-based data such as total rainfall depth. Considering the urban hydrological modeling capability, this study aimed to use Visual OTTHYMO v3.0 (VO3), the third version of the INTERHYMO – OTTHYMO hydrologic model simulation software package designed for Microsoft Windows OS [6]. It is a single event hydrologic model which simulates runoff from single storm events. The model is an appropriate design tool for use in projects such as watershed studies and stormwater management design [40]. The model includes four commands for four unit hydrograph options: STANDHYD - uses parallel standard instantaneous unit hydrographs for impervious and pervious areas of the catchment, and this method is recommended for modelling urban watersheds with greater than 20% impervious areas; NASHYD - uses the Nash instantaneous unit hydrograph method; WILHYD - uses the Williams and Hann (HYMO) unit hydrograph method; SCSHYD - uses the Nash hydrograph method based on SCS parameters and with N being five reservoirs. The routing routines available to calculate the transformation of a streamflow hydrograph are based on the continuity equation and a storage discharge relation. The routines use variable storage coefficient method, Muskingum-Cunge and storage-indication method [7]. This study used an existing model of the study area developed for current landuse conditions using Visual OTTHYMO v3.0, and the model of the study area was obtained from the Credit Valley Conservation. The model contains 9 sub-catchment areas (shown in the Figure 2) with a total area of 478.66 ha, 6 sub-catchments were modeled using standard instantaneous unit hydrographs (the total impervious areas of which varies from 39% to 84%), and other 3 sub-catchments were modeled using Nash instantaneous unit hydrograph. The rainfall losses were computed by means of modified curve number procedures. The routing routine used for channel and pipe was variable storage coefficient method, and for the storage area was storage-indication method. The 24 hour duration storm depths of 2, 5, 10, 25, 50 and 100 year return for observed and future (six RCM+GCM pairs and average of six pairs) for case 1 were used as input in the hydrologic model for flow simulation. The design storm depths were discretized by using Chicago distribution as described in the previous section to input as design hyetographs in hydrological model. The 24 hour design storms used for flow simulation are listed in Table 4.

Table 4. Design storm depths (in mm) used for flow simulation

Return Period	Obse-rved	Crcm Ccsm	Crcm Cgcm	Hrm3 Gfdl	Hrm3 Hadcm3	Rcm3 Cgcm3	Rcm3 Gfdl	Aver -age
2	45.3	49.7	50.3	57.8	41.5	56.3	57.8	52.2
5	58.7	64.8	66.2	81.6	58.4	75.1	71.6	69.6
10	68.9	76.5	77.0	104.6	74.8	89.6	82.5	84.2
25	83.7	93.0	91.1	145.2	101.0	111.5	100.1	107.0
50	96.0	107.1	101.4	185.9	124.5	130.1	116.3	127.5
100	109.6	122.4	111.9	238.7	151.7	151.2	135.8	151.9

3.3. Hydraulic Modeling

The Hydrologic Engineer Center's River System Analysis System (HEC-RAS) software [24], that allows to perform one-dimensional steady and unsteady flow river hydraulics calculations, were used for flooding scenario analyses under future climate condition in the floodplain of Clearview Creek. The system includes a graphical user interface, separate hydraulic analyses components, data storage and management capabilities, graphic and reporting facilities. HEC-RAS is capable of modelling a full network of natural or constructed channels. HEC-RAS requires the input of geometric data to represent river network/reach, channel cross-section data, and hydraulic structure data such as bridge and culvert data.

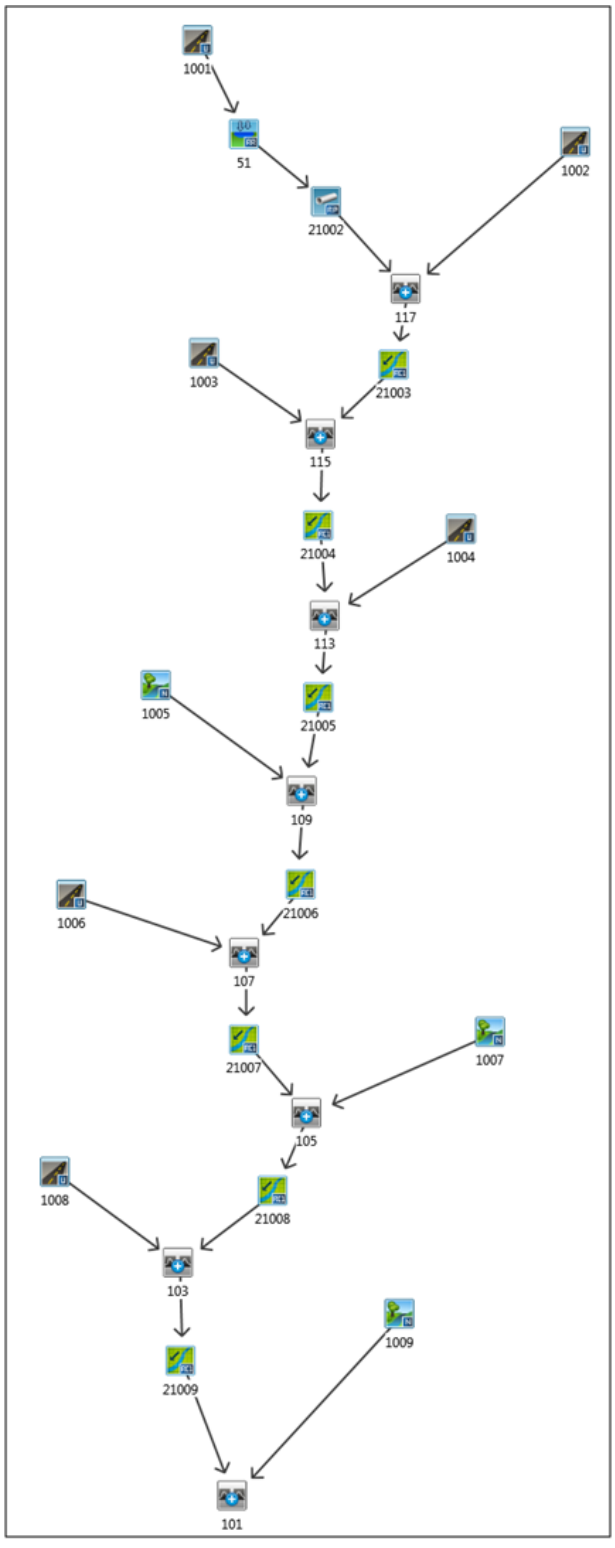

Figure 2. Hydrologic model schematic for Clearview Creek catchment

The length of Creek modeled in this study is 2878m. The model includes 45 cross-sections and 4 culverts as

shown in the Figure 3. The cross-section number started with 0 at the outlet of Creek on the shore of the Lake, and the river stations were numbered as the distance from the outlet. The cross-section data, high cord and low cord elevations for culverts were generated from a high resolution digital terrain model (DTM) by using HEC-GeoRAS [23]. HEC-GeoRAS, an extension for use with ArcGIS tools, specifically designed to process geospatial data for use with HEC-RAS. It enables the hydraulic engineers to create a HEC-RAS import file containing geometric data from a digital terrain model (DTM), process water surface profile data exported from HEC-RAS, and perform floodplain mapping. A 1m x 1 m resolution DTM was developed employing ArcGIS and using a 5m x 5m resolution DTM of the entire catchment area and recent survey data adjacent to the Creek obtained from Credit Valley Conservation. A 1m x 1 m resolution DTM was prepared using the survey data, existing 5m x 5m resolution DTM was resampled to 1m x 1 m resolution DTM, and finally mosaic 1m x 1 m resolution DTM was created using DTM from survey data as mosaic operator. Then, a RAS GIS file that contains cross-section elevations with bank station data, and high cord and low cord elevations for culverts was generated from the mosaic DTM using HEC-GeoRAS. The geometric data, hydraulic structure and flow data were completed in HEC-RAS. The Manning's roughness coefficient values, expansion and contraction coefficients for the cross-sections were completed following the Credit Valley Conservation's technical guideline [9] for hydrologic and hydraulic analyses. The detail survey data for the culverts (location, dimensions, length, height from obvert to top of road, photos etc.) were also obtained from the Credit Valley Conservation. Some buildings were set as obstructed area at cross-section of river stations 520, 2448, 2500 and 2545. As a mixed flow regime calculation was made, the boundary conditions were entered at both upstream and downstream ends of the Creek. For steady flow boundary condition, the known water surface elevation, mean annual water surface elevation (74.8m) for Lake Ontario at Mississauga [9] was entered at downstream end, and critical depth was selected as upstream boundary condition at river station 2878. The peak flows simulated for 24 hour storm depths listed in Table 4 were used as input in the HEC-RAS model. The peak flows at the hydrologic elements 117, 115, 113, 109, 107, 105, 103 and 101 of the hydrologic model (shown in Figure 2) were entered at the river station 2878, 2672, 2297, 1779, 1556, 1001, 419 and 0. The peak flow values of observed/baseline, 6 RCM+GCM pairs and average of six pairs for steady flow simulation are listed in the Table 5.

Table 5. Peak flows (m3/s) used for steady flow simulation in HEC-RAS

	RS	2yr	5yr	10yr	25yr	50yr	100yr		RS	2yr	5yr	10yr	25yr	50yr	100yr
Observed\baseline	2878	4.15	6.21	13.07	23.16	31.45	37.95	Future average	2878	5.19	13.61	23.52	36.61	49.79	64.33
	2672	5.14	7.23	13.26	23.28	31.45	38.53		2672	6.19	13.80	23.60	36.50	50.81	65.79
	2297	5.77	8.24	13.29	23.34	31.47	38.57		2297	7.02	13.84	23.66	36.84	50.88	66.03
	1779	4.43	6.64	10.82	17.77	23.72	29.07		1779	5.55	11.19	18.01	28.02	37.60	49.52
	1556	5.41	8.28	11.51	18.78	25.01	30.44		1556	6.94	11.91	19.03	29.33	39.19	51.03
	1001	5.25	7.91	12.22	19.51	25.64	31.20		1001	6.58	12.62	19.75	30.10	39.92	51.70
	419	6.27	9.34	12.79	20.22	26.54	32.27		419	7.93	13.21	20.47	31.11	41.11	53.01
	0	6.42	9.57	13.00	20.55	26.97	32.78		0	8.12	13.45	20.81	31.63	41.77	53.83
CrcmCcsm	2878	4.81	10.18	18.16	29.54	36.58	46.44	CrcmCgcm	2878	4.91	11.20	18.47	28.24	35.07	39.33
	2672	5.77	10.47	18.27	29.58	36.47	47.21		2672	5.87	11.43	18.59	28.41	35.05	40.00
	2297	6.55	10.52	18.33	29.67	36.82	47.43		2297	6.65	11.48	18.66	28.50	35.24	40.09
	1779	5.14	8.90	14.33	22.28	28.01	35.08		1779	5.24	9.56	14.56	21.37	26.29	30.10
	1556	6.44	9.56	15.20	23.52	29.33	36.74		1556	6.55	10.23	15.43	22.56	27.61	31.53
	1001	6.08	10.26	15.91	24.18	30.11	37.34		1001	6.20	10.94	16.13	23.21	28.29	32.26
	419	7.36	10.79	16.49	25.05	31.13	38.57		419	7.50	11.67	16.73	24.09	29.21	33.37
	0	7.53	11.02	16.76	25.46	31.64	39.19		0	7.66	11.66	17.00	24.49	29.69	33.91
Hrm3Gfdl	2878	6.07	21.77	35.10	60.86	86.54	115.37	Hrm3Hadcm3	2878	3.59	6.16	17.03	34.90	48.06	64.20
	2672	7.10	21.82	35.27	62.19	88.40	117.64		2672	4.55	7.18	17.17	34.87	48.83	65.66
	2297	8.07	21.87	35.43	62.35	89.05	118.25		2297	5.20	8.18	17.24	35.05	48.91	65.90
	1779	6.49	16.78	26.89	46.51	66.72	89.87		1779	3.82	6.59	13.56	26.15	36.19	49.42
	1556	8.10	17.76	28.20	48.01	68.60	92.61		1556	4.72	8.22	14.38	27.46	37.86	50.93
	1001	7.73	18.49	29.00	48.53	69.60	94.72		1001	4.60	7.85	15.09	28.14	38.50	51.60
	419	9.14	19.15	29.97	49.87	71.21	97.16		419	5.46	9.27	15.66	29.04	39.68	52.90
	0	9.36	19.47	30.47	50.66	72.29	98.68		0	5.59	9.50	15.91	29.53	40.31	53.73
Rcm3Cgcm3	2878	5.81	17.25	27.24	39.40	51.30	63.90	Rcm3Gfdl	2878	6.07	14.89	22.26	34.30	42.35	54.74
	2672	6.82	17.36	27.41	40.03	52.40	65.37		2672	7.10	15.05	22.42	34.28	42.82	55.83
	2297	7.76	17.43	27.50	40.11	52.41	65.59		2297	8.07	15.10	22.48	34.46	43.01	56.10
	1779	6.21	13.69	20.64	31.06	38.97	49.19		1779	6.49	12.09	17.20	25.72	32.21	41.63
	1556	7.77	14.52	21.79	31.47	40.46	50.70		1556	8.10	12.87	18.19	27.08	33.64	43.17
	1001	7.38	15.23	22.48	32.20	41.23	51.35		1001	7.73	13.57	18.92	27.77	34.33	43.81
	419	8.78	15.81	23.36	33.30	42.40	52.66		419	9.14	14.13	19.61	28.66	35.53	45.10
	0	8.99	16.06	23.73	33.83	43.08	53.48		0	9.36	14.39	19.93	29.14	36.11	45.80

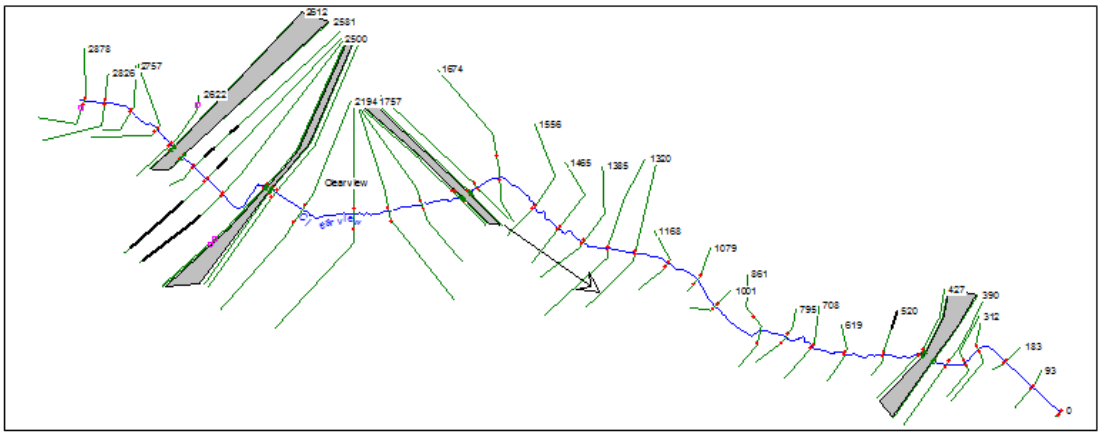

Figure 3. Geometric data schematic showing cross-section and culvert locations

4. Results and Discussion

4.1. Design Storm

Frequency analyses were performed on a total of 52 annual maximum time series including 4 observed, 24 NARCCAP current and 24 NARCCAP future dataset. The best fitted distribution among twenty seven distributions for annual maximum time series of four durations for NARCCAP current and future datasets are listed in the Table 1. Among the 96 selection for 48 NARCCAP datasets shown in the Table 2, L-Moment GEV Min was selected 15 times (the highest), that is 15.6% of the total selection and Gumbel EV1 Max was selected for 11 times that is 11.5% of the total selection. This reveals the importance of selection of appropriate distribution for calculation of storm depths considering climate change impact. The storm depths calculated from observed data and NARCCAP datasets are presented in Table 2. The delta change factor was applied to get the storm depths under future climate condition. The storm depths for all six RCM+GCM pairs show a significant increase in the future. All the data in the Table 2 are plotted as scatter plot on a graph (Figure 4) whose abscissa and ordinate are the values observed and NARCCAP future storm depths respectively. The abscissa and ordinate are plotted on the same scale and 45 degree line is drawn to facilitate interpretation of the scatter plot. The linear trendlines including the trendline equations and the dispersion of data (indicated by the R^2 values) above the 45-degree line reveal that the increase of storm depths under future climate is higher for higher values. The higher values of storm depths may either represent storm depths for higher return period or higher duration. The linear trendlines also show that the overall increase in storm depths is highest for case 1 (when the distributions were identified by Chi-square test), and lowest for case 3 (when frequency analyses was performed using Gumbel EV1 Max).

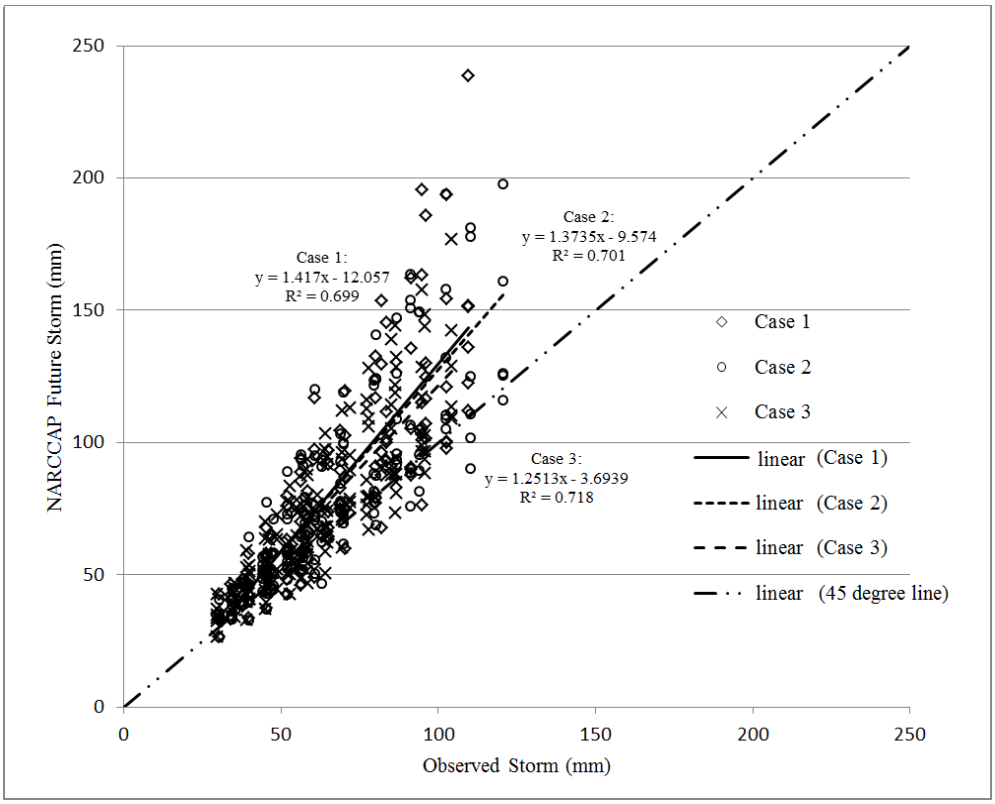

Figure 4. Scatterplot of design storm depths calculated from observed data and NARCCAP future datasets

The percentage difference between storm depths calculated from observed data and NARCCAP future averages for four durations and six return periods are presented in the Figure 5, Figure 6 and Figure 7. These figures show significant increase of storm depths for all durations and return period; overall, the storm depths increase with the increase in return period. For example, storm depths of 24 hour duration for 2yr, 25yr and 100yr return period increased by 15.3%, 27.8% and 38.6% for case 1; 15.8%, 27.7% and 36% for case 2 and 18.4%, 22.8% and 24.6% for case 3. These figures also show that the storm depths increase with the increase in duration overall. For example, storm depths of 2yr return period for 3hr, 6hr, 12hr, 24hr duration increased by 12.1%, 13.2%, 14.3% and 15.3% for case 1; 11.9%, 12.2%, 14.5% and 15.8% for case 2 and 15.3%, 15.2%, 16.5% and 18.4% for case 3. The highest increase of 38.6% was observed for 24hour duration and 100 year return period storm depths for case 1. Therefore, the storm depths calculated in case 1 will be used as input in the hydrological model for flow simulation. The box plots in the Figure 8 shows the relative change (ratio of NARCCAP future storm depths of 6 RCM+GCM models and storm depths from observed data)) of storm depths for different durations and return period. It is revealed from the figure that the variability of relative change increase with an increase in return period and decrease with an increase in storm duration overall.

The overall uncertainty of the design storm for NARCCAP climate data was assessed using the co-efficient of variation (CV). For a given duration and return period, CV is calculated as the ratio between the standard deviation of NARCCAP storm depths to the corresponding mean values. CV was compared to assess the inter-model variability for different duration and return period for storm depths calculated from NARCCAP data sets under future climate conditions. The CV calculated for storm depths from 6 RCM+GCM pairs under future climate are presented in the Figure 9, Figure 10 and Figure 11. Overall the variability increases with an increase in return period and decrease with an increase in duration. For example, CV of 24 hour duration for 2yr, 25yr and 100yr return period are 11.2%, 17.1% and 27.2 % for case 1; 8%, 18.3% and 30.4% for case 2 and 9.7%, 17.2% and 18.4% for case 3. The CV of 2yr return period for 3hr, 6hr, 12hr, 24hr duration are 14%, 12.3%, 9.1% and 11.2% for case 1, 12.4%, 10.5%, 9.3% and 8.3% for case 2, and 13.9%, 11.5%, 10.9% and 9.7% for case 3.

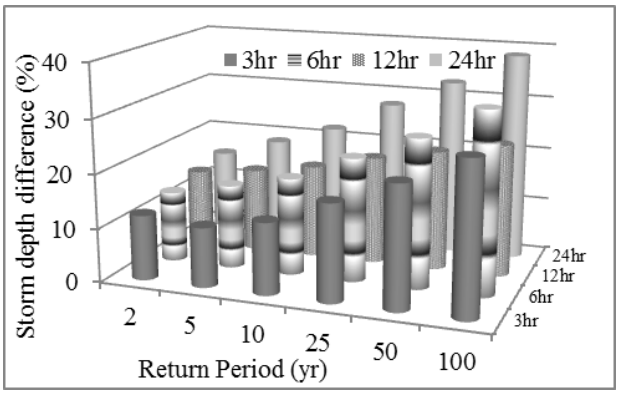

Figure 5. Difference between observed and NARCCAP future average storm depths for case 1

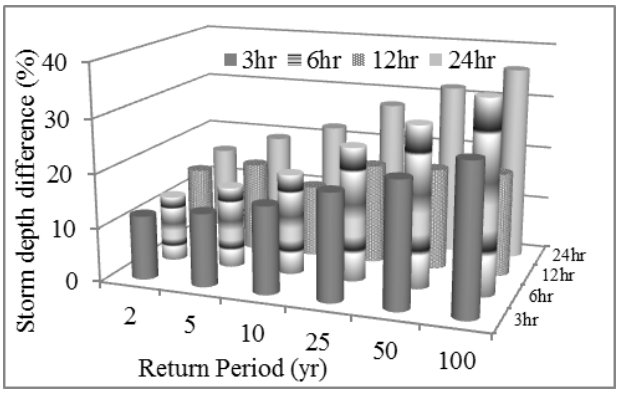

Figure 6. Difference between observed and NARCCAP future average storm depths for case 2

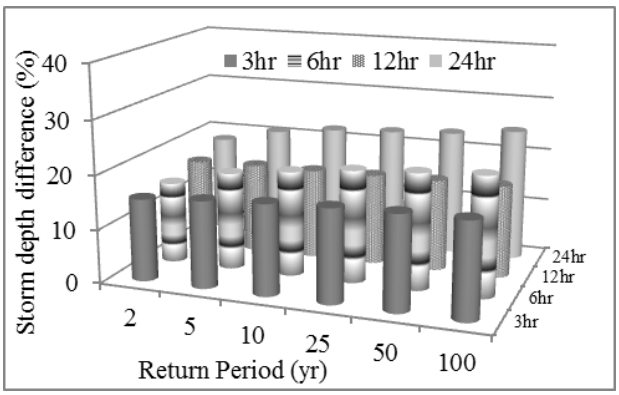

Figure 7. Difference between observed and NARCCAP future average storm depths for case 3

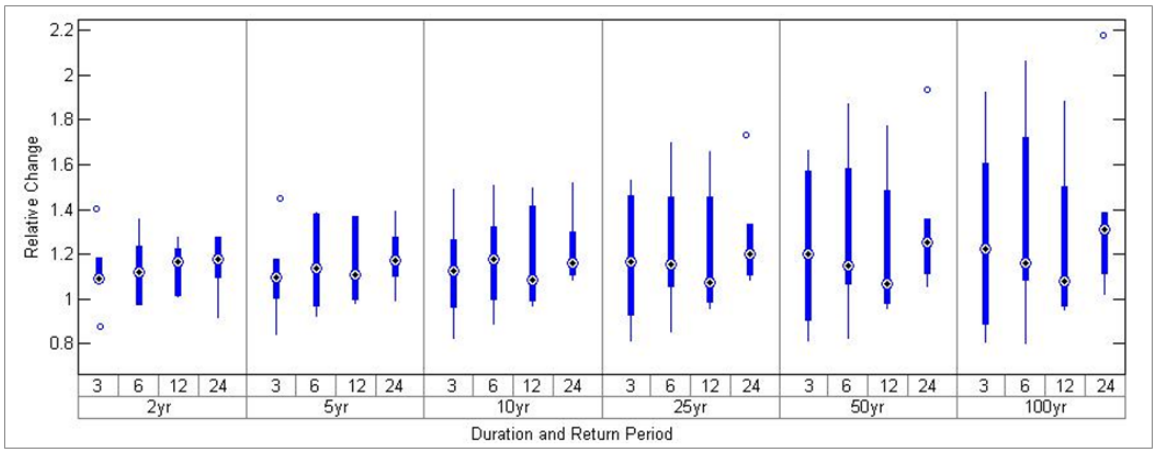

Figure 8. Box-plots of relative change calculated from observed and NARCCAP future storm depths

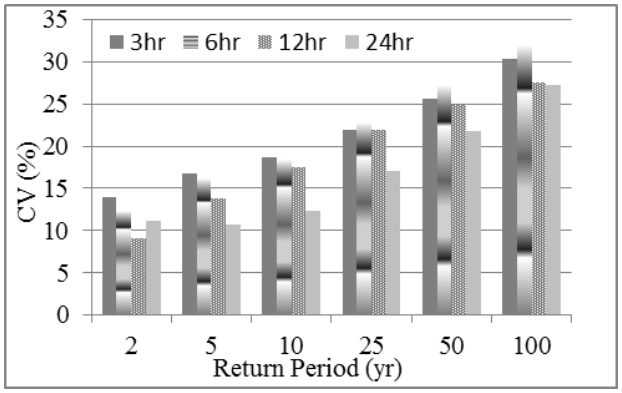

Figure 9. Comparison of CV of future storm depths for different return period and duration for case 1

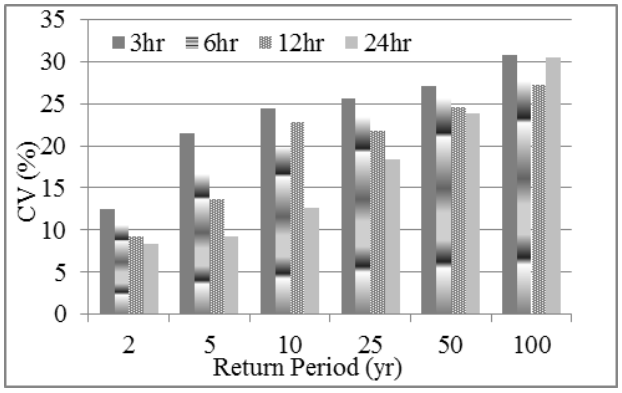

Figure 10. Comparison of CV of future storm depths for different return period and duration for case 2

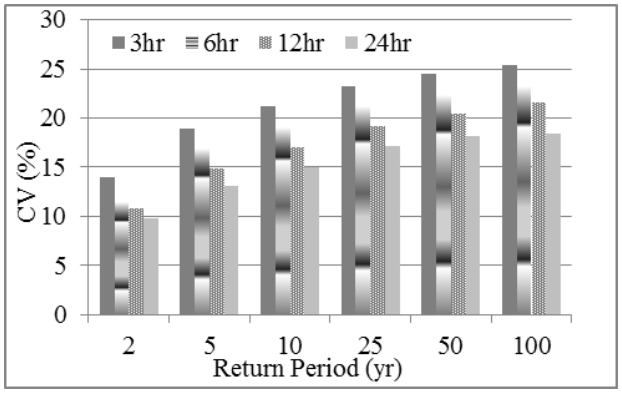

Figure 11. Comparison of CV of future storm depths for different return period and duration for case 3

4.2. Storm Flow

The increase in flows under future climate condition (difference between flows from observed and NARCCAP future average storms of 24 hour duration) at hydrologic element 101, 1003 and 1005 are presented in Figure 12. The hydrologic element 101 is the outlet of the catchment, and 1003 and 1005 are two sub-catchments with nearly same area of 23.26 and 25.82 ha. The sub-catchment 1003 was modeled as a highly urbanized area using standard instantaneous unit hydrographs as its total impervious area is about 84% , and the sub-catchment 1005 was modeled as a rural catchment using Nash instantaneous unit hydrograph. Analysis of flows at the outlet presents the hydrologic impact on the entire watershed, and the analysis of flows at two sub-catchments represent the response of climate impact in catchment with different landuse conditions. Flows from observed and NARCCAP future average storms at the outlet and two sub-catchments are presented in Figure 13, 14 and 15. Like increase in storm depths, percentage differences of the peak flow increase with an increase in return period overall. For example, increase of peak flows for 2yr, 25yr and 100 yr return period are 26.46%, 53.94% and 64.22% at the outlet, 21.69%, 32.93% and 51.61% for the sub-catchment area 1003, and 30.41%, 44% and 56.13% for the sub-catchment area 1005. The analyses of storm depths and peak flow results revealed that the percentage increase in peak flows are much higher than that of storm depths under future climate condition. The increase of storm depths of 24 hour duration and 2yr, 25yr and 100yr return period are 15.3%, 27.8% and 38.6%, those are 26.46%, 53.94% and 64.22% for peak flow at the outlet of the catchment. It is shown in Figure 14 and Figure 15 that the peak flows in the sub-catchment 1003 are much higher than the peak flows in the sub-catchment 1005. This is a common phenomenon that area with higher impervious area produces a higher peak flow. Figures 14 and 15 present that the peak flows for 2yr, 25yr and 100yr return period in sub-catchment 1003 are 2.72 m^3/s, 5.85 m^3/s and 7.87 m^3/s for baseline scenario and 3.31 m^3/s, 7.78 m^3/s and 11.93 m^3/s for future scenario; those are 0.22 m^3/s, 0.62 m^3/s and 0.93 m^3/s for baseline scenario and 0.28 m^3/s, 0.9 m^3/s and 1.45 m^3/s for future scenario in sub-catchment 1005. However, it is shown in Figure 12 that increase in peak flows under future climate condition in sub-catchment 1005 is higher than that in the sub-catchment 1003 - increase in storm depths of 24 hour duration and 2yr, 25yr and 100yr return period in the sub-catchment 1003 are 21.69%, 32.93% and 51.61 %, and the increases are 30.41%, 44% and 56.13 % in the sub-catchment 1005. The box plots in Figure 8 shows the relative change (NARCCAP future storm depths/observed storm depths) of storm depths for different durations and return periods. It is revealed from the figure that the variability of relative change increase with an increase in return period and decrease with an increase in storm duration overall. The box plots in Figure 16 shows the relative change (ratio of future peak flow from NARCCAP future storm depths of 6 RCM+GCM models and peak flow from observed storm depths) of storm depths for different return periods. It is revealed from the figure that the variability of relative change increases with an increase in return period overall if the outlier is also considered. Figure 8 and Figure 16 also show that the variability in relative change for peak flows is higher than the storm depths overall. The relative change of the 24 hour 100 year storm depths varies from 1.02 to 2.18 for six RCM+GCM data, and the relative change for flow of corresponding storms varies from 1.03 to 3.01.

Similar to storm depths, the overall uncertainty of the peak flows for NARCCAP climate data was assessed using the co-efficient of variation (CV). CV was compared to assess the inter-model variability of the peak flows resulted from 24 hour storm depths of different return period calculated from six RCM+GCM pair data sets under future climate conditions. The CVs calculated for peak flows at the outlet (101), and sub-catchments 1003 and 1005 are presented in Figures 17, 18 and 19. The CVs for storm depths are also presented in the Figures.

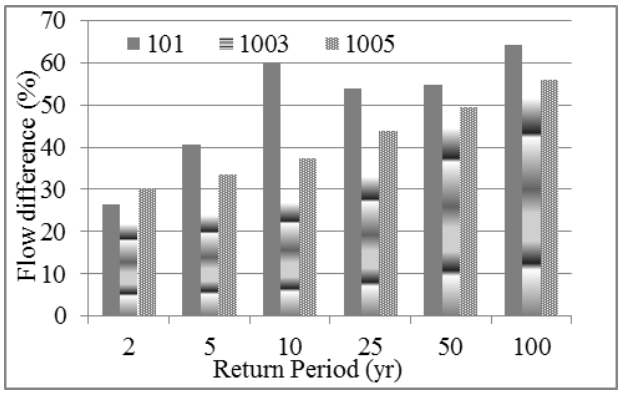

Figure 12. Flow difference for observed and NARCCAP future average storms

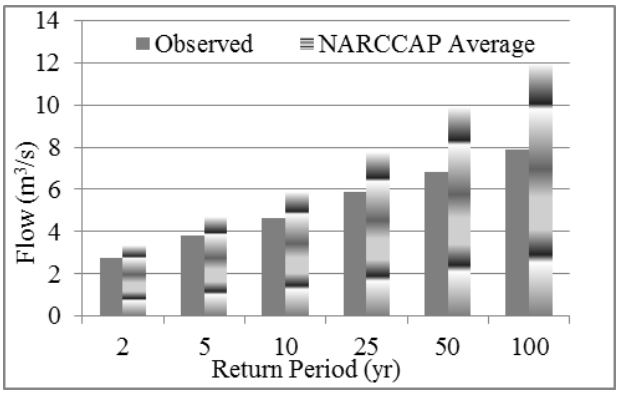

Figure 14. Flows from observed and NARCCAP future average storms at hydrologic element 1003

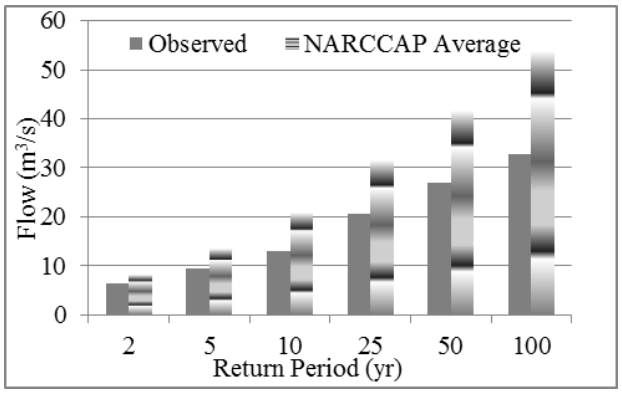

Figure 13. Flows from observed and NARCCAP future average storms at hydrologic element 101 (outlet of the catchment)

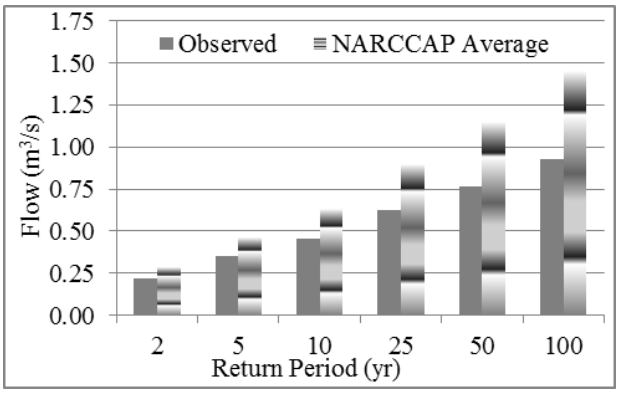

Figure 15. Flows from observed and NARCCAP future average storms at hydrologic element 1005

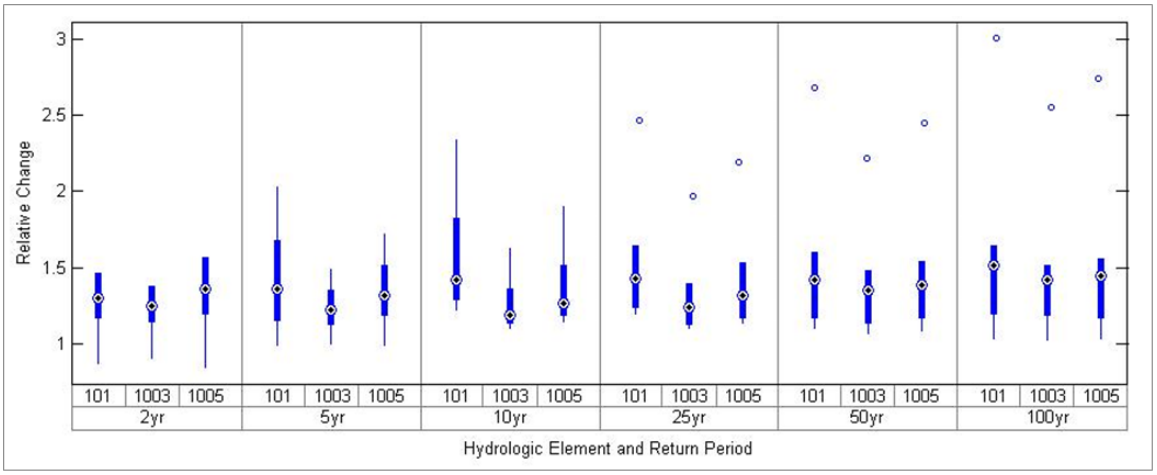

Figure 16. Box-plots of relative change of flows from observed and NARCCAP future storm depths

Like the storm depths, the variability of the peak flow increases with an increase in return period. Figures 17, 18 and 19 show that the variability of peak flows are much higher than that of storm depths. The CV for peak flows of 100 year return period are 39.1%, 32.5% and 35.7% in the outlet, the sub-catchment 1003 and the sub-catchment 1005, respectively, and the CV for 24hour storm of 100 year return period is 27%. The figures also show that the variability is higher in case of the sub-catchment 1005 than in case of the sub-catchment 1003- the CV for 2 yr, 25yr and 100yr return period are 19.8%, 24.8% and 35.7% respectively in the sub-catchment 1005, those are 13.9%, 21.9% and 32.5% respectively in the sub-catchment 1003.

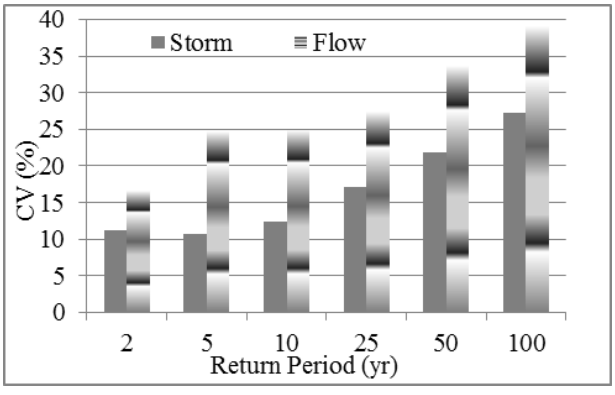

Figure 17. CV of future storm depths and flows for 24 hour storms at hydrologic element 101 (outlet of the catchment)

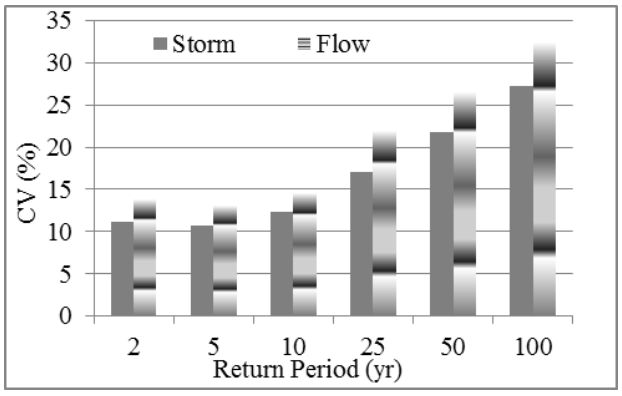

Figure 18. CV of future storm depths and flows for 24 hour storms at hydrologic element 1003

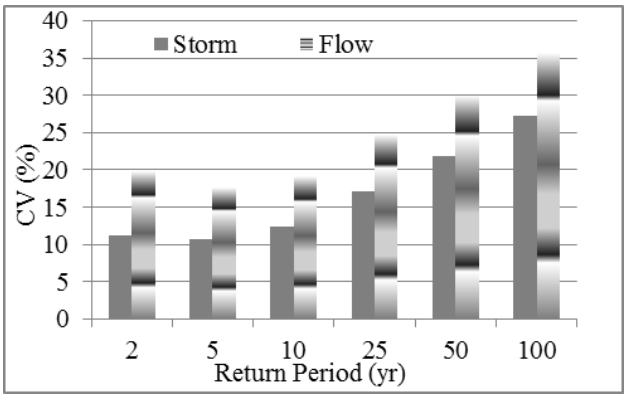

Figure 19. CV of future storm depths and flows for 24 hour storms at hydrologic element 1005

4.3. Hydraulic Analyses

The hydraulic metrics –water surface (W.S.) elevation, top width (top widths of the wetted cross section) and area (flow area of the entire cross-section including ineffective flow) were obtained from profile output table in HEC-RAS model and were used for the assessment of climate change impact on flooding. An increase in W.S. elevation and top widths represent an increase in flood inundation depth and extents under future climate condition. The increase of W.S. elevation and top widths are the differences of the values simulated for the flows resulted from the storm depths of observed data and averages of the six RCM+GCM pair climate data (listed in the Table 5). These metrics were analyzed for three stations – one near the most upstream of the Creek (river station 2674), one near the most downstream of the Creek (river station 357) and one in the middle of the Creek (river station 1665) and the results are shown in Figure 20. Increase in W.S. elevation and top widths were also calculated for all 45 cross-sections and averages (average of the increases at 45 cross-sections) are shown Figure 20. This figure shows that increase in W.S. elevation and top widths varies significantly among the cross sections. The increase in W.S. elevation for 2yr, 25 yr and 100 yr return period flow are 6cm, 13cm and 20 cm at river station 2674 ; 12cm, 45 cm and 67 cm at river station 357; and 7cm, 21cm and 28cm at river station 1465 respectively. The increase in top widths for 2yr, 25 yr and 100 yr return period flow are 8.2m, 21.9m and 39m at river station 2674;0.4m, 4.4 m and 124.7m at river station 357; and 5.5 m, 7.7m and 10.5m at river station 1465 respectively. The only reason of this variation is the shape of the cross-section. Average of increase in W.S. elevation and top widths of all cross sections show overall increase of inundation depths and extent along the Creek. The increase in W.S. elevation for 2yr, 25 yr and 100 yr return period flow are 6 cm, 22cm and 30cm respectively, and the increase in top widths are 4m, 23.7m and 37.1 m respectively. A map showing the flood line for 100 year return period flood for the current period and future period is presented in Figure 21. The blue and red line represents the flood line for the 100 year return period flow from observed data and average of six NARCCAP RCM+GCM pairs data sets respectively.

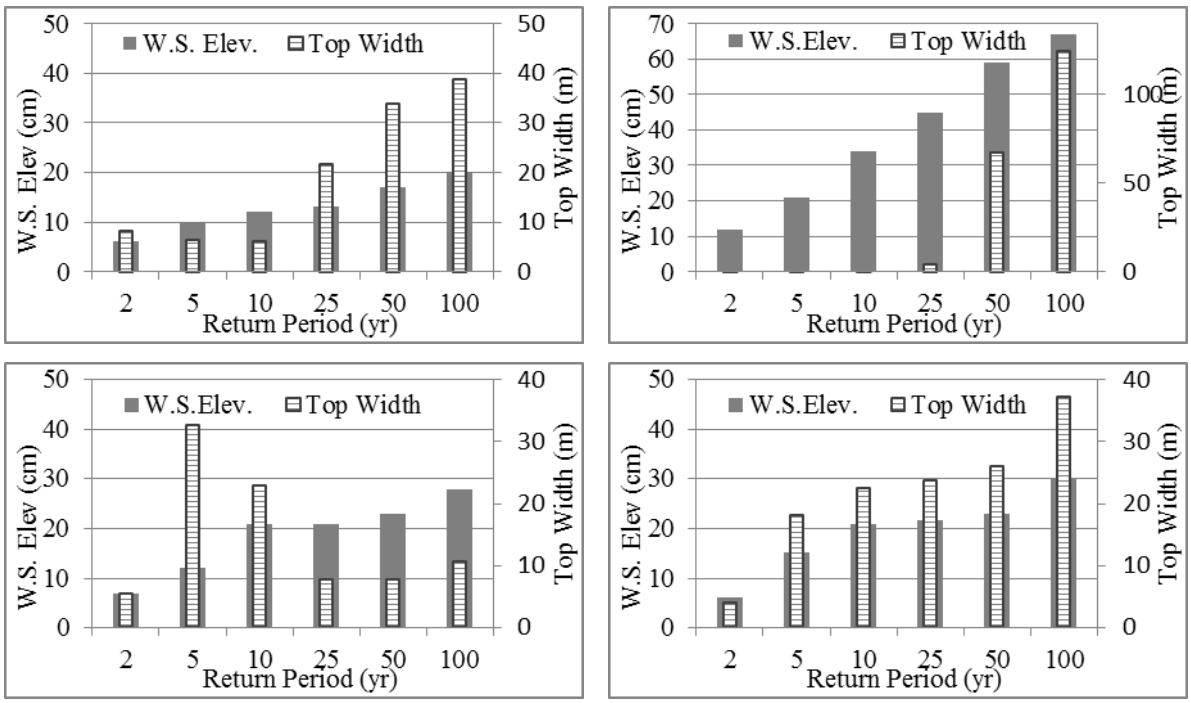

Figure 20. Increase of W.S. elevation and top width (top left, top right, bottom left and bottom right represent station 2674, 357, 1465 and average of 45 stations) along the Creek

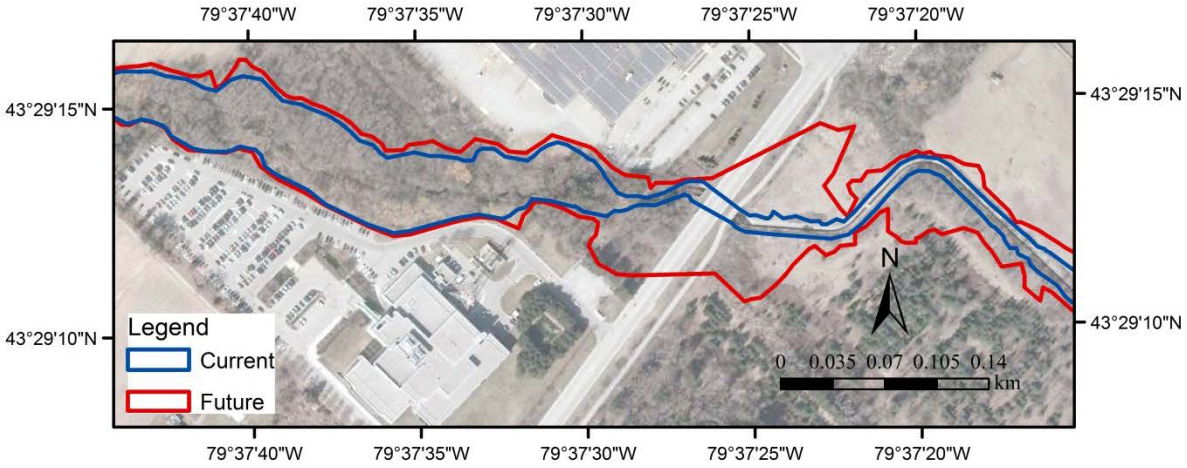

Figure 21. Flood line map for a section of Clearview Creek (orthophoto courtesy of the Credit Valley Conservation)

The CVs of flow area for six RCM+GCM pair data under future climate were calculated for all 45 cross-sections and averages (average of the CVs at 45 cross-sections) and are shown Figure 22. The CVs for 24hr return period storms and corresponding flows at the outlet for different return period are also presented in Figure 21. The figure shows that the variability of flow area is much higher than the variability of storm depths, but the differences among variabilities in flow and in flow area are very small overall. For example, the CVs for 100 year return period stom depths, flows and flow area are 27.2%, 39.1% and 39.4 % respectively.

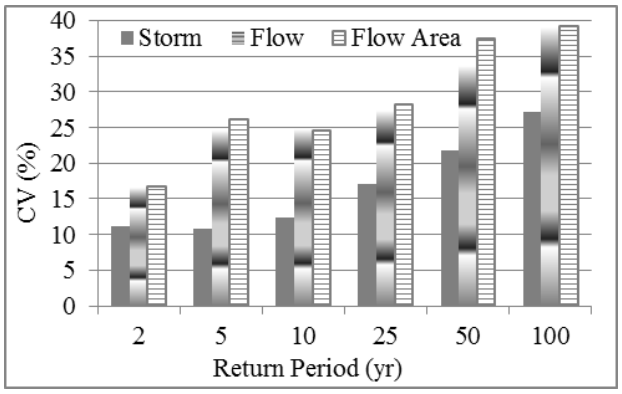

Figure 22. CV of storm depths, flows at outlet and average of flow areas at all cross-sections

5. Conclusions

This study investigated the climate change impact on design storms, peak flows and flooding scenario using NARCCAP climate simulations based on A2 emission scenario described in the Special Report on Emissions Scenarios (SRES) for Clearview Creek drainage area located in Southern Ontario, Canada. A statistical analysis software, Hydrognomon, hydrologic modeling tool Visual OTTHYMO and a river system analyses tool HEC-RAS were used for design storm depth calculation, simulation of flows and hydraulic metrics. The procedure followed and the findings of this study are concluded as follows:

Frequency analysis was performed on data from six RCM+GCM pairs by using the best fitted distribution among twenty seven distributions. Pearson chi-square test and Kolmogorov-Smirnov were used to test the goodness of fit of each distribution. L-Moment GEV Min was selected 15.6% of the total selections for NARCCAP data sets. The linear trendlines show that the overall increase of storm depths is highest when the distributions were identified by Chi-square test (case 1). The percentage increase (difference of average of storm depth from six model and observed data) for 24hr100yr storm depths is also highest for case 1. The storm depths of case 1 were used for flow simulation. A novel finding of this study is that there is a significant increase in storm depths for all durations and return period under future climate conditions, and the percentage increase in storm depth increases with an increase in return period and duration.

Peak flows using 24 hours storms of different return period were analysed, and the results show that the peak flow increase with a range of 26 % to 64% for 2yr and 100yr return period at the outlet of the Creek. Results also revealed that the peak flows from a catchment with higher impervious area are much higher than that for a catchment with a low impervious area, but the percentage increase in peak flows under future climate condition is less in a catchment with higher impervious area. The percentage increases of peak flows are much higher than that of storm depths under future climate condition.

Higher peak flows will result in increased flood inundation depths and extents in the Clearview Creek catchment area. Analysed hydraulic metrics simulated by HEC-RAS show an average increase in water surface elevation and extents (top widths of wetted cross sections) are 30 cm and 37.1 m for a 100 year return period flood overall. The spatial variability of the metrics along the Creek is very significant due to the shape of the cross sections. The increases in the metrics for other return period are also noteworthy.

The analysed CV values indicate that variability of flow simulated by Visual OTTHYMO and flow area simulated by HEC-RAS are much higher than the variability of the storm depths under future climate condition, and the difference between flow and flow area variability is insignificant overall. The box plot results indicate that the variability of relative change of storm depths increase with an increase in return period, and variability of relative change of storm depths decrease with the increase of duration. The box plot results also indicate that the variability in relative change for peak flows is higher than the storm depths overall.

The changes in urban stormwater runoff resulting from the effect of climate change will have important implication for selecting approaches for urban flood management measures. This study provides some information and knowledgebase that could be used for future development in the Clearview Creek catchment area as well as other Lake Ontario tributaries of similar characteristics.

Acknowledgement

We wish to thank the North American Regional Climate Change Assessment Program (NARCCAP) for providing the data used in this paper. The authors acknowledge the Credit Valley Conservation and Environment Canada for providing data and models for the study area. This study was supported by the Natural Science and Engineering Research Council of Canada (NSERC) discovery grant.

References

[1] Bates, B., Kundzewicz, Z.W., Wu, S., and Palutikof, J., "Climate change and water," Technical Paper of the Intergovermental Panel on Climate Change. Geneva: IPCC Technical Paper VI, 2008.

[2] Berggren,K., Olofsson, M.,Viklander, M., Svensson, G., and Gustafsson, A., "Hydraulic Impacts on Urban Drainage Systems due to Changes in Rainfall Caused by Climatic Change," J. Hydrol. Eng., 17 (1), 92-98, 2012.

[3] Brown, C., "The end of reliability." J. Water Resour. Plann. Manage., 136(2), 143-145, 2010.

[4] Chen, C., and Knutson, T., "On the verification and comparison of extreme rainfall indices from climate models." J. Clim., 21 (7), 1605-1621, 2008.

[5] City of Mississauga, Development requirement manual. City of Mississauga, Mississauga, Ontario, Canada, 2009.

[6] Civica Infrastructure, Visual OTTHYMO (VO) v3.0 User's Guide, Civica Infrastructure Inc., Vaughan, Ontario, Canada, 2013.

[7] Civica Infrastructure, Visual OTTHYMO (VO) v3.0 Reference Manual, Civica Infrastructure Inc., Vaughan, Ontario, Canada, 2012.

[8] Collins W.D., Bitz, C.M., Blackmon, M.L., Bonan, G.B., Bretherton, C.S., Carton, J.A., Chang, P., Doney, S.C., Hack, J.J., Henderson, T.B., Kiehl, J.T., Large, W.G., McKenna, D.S., Santer, B.D., and Smith, R.D., "The community climate system model version 3 (CCSM3)," J. Climate, 19: 2122-2143, 2006.

[9] Credit Valley Conservation (CVC), CVC standard parameters, 2011. Retrieved from http://www.creditvalleyca.ca/wp-content/uploads/2011/09/020-Standard-Parameters-Appendix-B.pdf (accessed 12 December 2015)

[10] Cunderlik, J.M., and Simonovic, S.P., "Inverse Flood Risk Modelling under Changing Climatic Condition," Hydrological Processes, 21(5), 563-577, 2007.

[11] Dibike, Y.B., & Coulibaly, P., "Validation of hydrological models for climate scenario simulation: the case of Saguenay watershed in Quebec," Hydrological Processes, 21(23), 3123-3135, 2007.

[12] Elguindi, N., Bi, X., Giorgi, F., Nagarajan, B., Pal, J., Solmon, F., Rauscher, S., and Zakey, A., RegCM Version 3.1 User's Guide, Trieste, Italy, 2007.

[13] Environment Canada, Canadian climate normal, 1981-2010 staion data, 2015. Retrieved from http://climate.weather.gc.ca/climate_normals/results_1981_2010_e.html?stnID=5097&lang=e&StationName=Toronto&SearchType=Contains&stnNameSubmit=go&dCode=1 (accessed 11 October 2015)

[14] Eum, H., Sredojevic, D., and Simonovic, S.P., "Engineering procedure for the climate change flood risk assessment in the upper Thames River Basin," J. of Hydrol. Eng., 16, 608-612, 2011.

[15] Flato, G. M., "The Third Generation Coupled Global Climate Model (CGCM3)," 2005. Retrieved from http://www.ec.gc.ca/ccmac-cccma/default.asp?n=1299529F-1 (accessed 9 August 2015).

[16] Flood Damage Reduction Program (FDRP), 2015. Retrieved fromhttps://ec.gc.ca/eau-water/default.asp?lang=En&n=0365F5C2-1 (accessed 9 August 2015)

[17] Forsee, W.J., and Ahmad, S., "Evaluating urban storm-water infrastructure design in response to projected climate change," J. Hydrol. Eng., 16 (11), 865-873, 2011.

[18] Gellens, D., and Roulin, E., "Streamflow response of Belgian catchments to IPCC climate change scenarios," J. Hydrol. 210, 242-258, 1998.

[19] GFDL GAMDT (The GFDL Global Model Development Team), "The new GFDL global atmospheric and land model AM2-LM2: Evaluation with prescribed SST simulations," J. Climate, 17, 4641-4673, 2004.

[20] Giorgi, F., Marinucci, M.R., and Bates, G.T., "Development of second generation regional climate model (RegCM2) I: boundary layer and radiative transfer processes," Mon. Weather Rev., 121, 2794-2813, 1993.

[21] Gordon, C., Cooper, C., Senior, C.A., Banks, H., Gregory, J.M., Johns, T.C., Mitchell, J.F.B., and Wood, R.A., "The simulation of SST, sea ice extents and ocean heat transports in a version of the Hadley Centre coupled model without flux adjustments," Climate Dynamics ,16, 147-168, 2000.

[22] Hamlet, A.F., and Lettenmaier, D.P., "Effects of climate change on hydrology and water resources in the Columbia River basin," J. Am. Water Resour. Assoc. 35 (6), 1597-1623, 1999.

[23] Hydrologic Engineering Center (HEC), HEC-GeoRAS GIS Tools for Support of HEC-RAS using ArcGIS User'sManual. U.S. Army Corps of Engineers, Davis, CA, USA, 2011.

[24] Hydrologic Engineering Center (HEC), HEC-RAS River Analysis System, Hydraulic Reference Manual. U.S. Army Corps of Engineers, Davis, CA, USA, 2010.

[25] IPCC, "Climate Change 2014: Synthesis Report," Contribution of Working Groups I, II and III to the Fifth Assessment Report of the Intergovernmental Panel on Climate Change, Core Writing Team, Pachauri, P.K. and Meyer, L.A. (eds.), IPCC, Geneva, Switzerland, 151 pp., 2014.

[26] Jones, R., Noguer, M., Hassell, D., Hudson, D., Wilson, S., Jenkins, G., and Mitchell, J., "Generating high resolution climate change scenarios using PRECIS," Met Office Hadley Center, Exter, p 40, 2004.

[27] Karla, A., and Ahmad, S., "Using Oceanic-atmospheric oscillations for long lead time streamflow forecasting," Water Resour. Res., 45, W03413, 2009.

[28] Keifer, D.J., and Chu, H.H., "Synthetic Storm Pattern for Drainage Design," ASCE Journal of the Hydraulics Division, Vol. 83 (HY4), pp: 1332.1-1332.25, 1957.

[29] Kite, G.W., Application of a land class hydrological model to climate change. Water Resour. Res. 29 (7), 2377-2384, 1993.

[30] Kozanis, S., Christofides, A., and Efstratiadis, A., "Scientific documentation of the hydrogram software version 4," Athens, pp173, 2010.

[31] Kundzewicz, Z.W., Mata L.J., Arnell, N.W., D¨oll, P., Kabat, P., Jimenez, B., Miller, K.A.,Oki, T., Sen, Z., and Shiklomanov. I.A., Fresh water resources and their management. In Climate Change2007. Impacts, Adaptation and Vulnerability. Contribution of Working Group II to the Fourth Assessment Report of the Intergovernmental Panel on Climate Change, Parry ML, Canziani OF, Palutikof JP, VanDerLinde PJ, Hanson CE(eds). Cambridge University Press: Cambridge, UK; 173-210, 2007.

[32] Lemmon, D.S. and Warren, F.J., Climate Change Impacts and Adaption: A Canadian Perspective. Ottawa, Ontario, Canada: Natural Resources Canada, 2004.

[33] Leung, R.L., and Wigmosta, M.S., "Potential climate change impacts on mountain watersheds in the Pacific Northwest," J. Am. Water Resour. Assoc. 35 (6), 1463-1471, 1999.

[34] Mailhot, A., Beauregard,I., Talbot, G., Caya, D., and Biner, S., "Future changes in intense precipitation over Canada assessed from multi-model NARCCAP ensemble simulations," Int. J. Climato., 32, 1151-1163, 2012.

[35] Mailhot, A., Duchesne, S., Caya, D., and Talbot, G., "Assessment of future change in intensity-duration-frequency (IDF) curves for Southern Quebec using the Canadian Regional Climate Model (CRCM)," J. Hydrol., 347, 197-210, 2007.

[36] Mearns, L.O., et al., 2007, updated 2012. The North American Regional Climate Change Assessment Program dataset, National

Center for Atmospheric Research Earth System Grid data portal, Boulder, CO. Data downloaded 2015-07-07.

[37] Mearns, L. O., Gutowski, W.J., Jones, R., Leung, L.Y., McGinnis, S., Nunes, A.M.B. and Qian, Y., "A regional climate change assessment program for North America," EOS, 90 (36), 311-312, 2009.

[38] Milly, P.C.D., Betancourt, J., Falkenmark, M., Hirsch, R.M., Kundzewicz, Z.W., Lettenmaier, D.P., and Stouffer, R.J., "Climate change-stationary is dead: whither water management?" Science, 319 (5863), 573-574, 2008.

[39] Moglen, G.E., and Vidal,G.E.R., "Climate change impact and storm water infrastructure in the Mid-Atlantic region: design mismatch coming?" J. Hydrol. Eng., 19, 2014.

[40] MTO, Evaluation of Drainage Management Software, 2015. Retrieved from http://www.mto.gov.on.ca/english/publications/drainage/software/otthymo.shtml#WHATDOESITDO (accessed 12 December 2015).

[41] MTO, MTO Drainage management manual. Drainage and Hydrology Section, Ministry of Transportation, Ontario, Canada, 1997.

[42] Music, B., and Caya, D., "Evaluation of the hydrological cycle over the Mississippi River Basin as simulated by the Canadian regional climate model (CRCM)," J. Hydrometeor., 8, 969-988, 2007.

[43] Nakicenvoic, N., Davidson, O., Davis, G., Grübler, A., Kram, T., Rovere, E., Metz, M., Morita, T., Pepper, W., Pitcher, H., Sankovski, A., Shukla, P., Swart, R., Watson, R., and Dadi, Z., Special Report on Emissions Scenarios. A Special Report of Working Group III of the Intergovernmental Panel on Climate Change. Cambridge University Press Cambridge, 599, 2000.

[44] NARCCAP, North American Regional Climate Change Assessment Program, 2013. Retrieved from http://www.narccap.ucar.edu/ (accessed 26 January 2013).

[45] Olsson, J., Berggren, K., Olofsson, M., and Viklander, M., "Apply-ing climate model precipitation scenarios for urban hydrological assessment: A case study in Kalmar City, Sweden,"Atmos.Res., 92(3), 364-375, 2009.

[46] Ontario Ministry of Natural Resources (OMNR), Technical Guide - River and Stream Systems: Flooding Hazard Limit. Ontario Ministry of Natural Resources, Ontario, Canada, 2002.

[47] Pope, V.D., Gallani, M.L., Rowntree, P.R., and Stratton, R.A., "The impact of new physical parameterizations in the Hadley Centre climate model—HadAM3," Climate Dynamics, 16, 123-146. 2000.

[48] Prudhomme, C., Reynard, N., and Crooks, S., "Downscaling of global climate models for flood frequency analysis: Where are we now?" Hydrol. Processes, 16(6), 1137-1150, 2002.

[49] Semadeni-Davies, A., Hernebring, C., Svensson, G., and Gustafsson, L., "The impacts of climate change and urbanisation on drainage in Helsingborg, Sweden: Combined sewer system," J. Hydrol., 350, 100-113, 2008.

[50] Valipour, M., "Optimization of neural networks for precipitation analysis in a humid region to detect drought and wet year alarms," Meteorological Application, 2015.

[51] Valipour M., "Long-term runoff study using SARIMA and ARIMA models in the United States," Meteorological Application, 22, 592-598, 2015.

[52] Valipour, M., "Use of surface water supply index to assessing of water resources management in Colorado and Oregon, US," Advances in Agriculture, Sciences and Engineering Research, 3(2):631-640, 2013.

[53] Valipour, M., "Estimation of Surface Water Supply Index Using Snow Water Equivalent," Advances in Agriculture, Sciences and Engineering Research, 3(1): 587-602, 2013.

[54] Zahmatkesh, Z., Karamouz, M., Goharian, E., and Burian, S.J., "Analyses of the effects of climate change on urban storm water runoff using statistically downscaled precipitation data and a change factor approach," J. Hydrologic Eng., 20(7), 05014022. 2015.

[55] Zhu, J., "Impact of climate change on extreme rainfall across the United States," J. Hydrol. Eng., 18(10), 1301-1309, 2013.

[56] Zhu, J., Stone, M.C., and Forsee, W., "Analysis of potential impact of climate change on intensity-duration-frequency (IDF) relationships for six regions in the United States," J. Water and Climate Change, 3(3), 185-196, 2012.